Radiology

Myeloperoxidase Molecular MRI Reveals Synergistic Combination Therapy in Murine Experimental Autoimmune Neuroinflammation

Anning Li, MD • Yue Wu, MD • Benjamin Pulli, MD • Gregory R. Wojtkiewicz, MSc • Yoshiko Iwamoto, BSc • Cuihua Wang, PhD • Jing-Hui Li, MD • Muhammad Ali, MBBS • Xiaoyuan Feng, MD • Zhenwei Yao, MD • John W. Chen, MD, PhD

From the Center for Systems Biology, Massachusetts General Hospital and Harvard Medical School, 185 Cambridge St, Boston, Mass 02114 (A.L., Y.W., B.P., G.R.W., Y.I., C.W., J.L., M.A., J.W.C.); Institute for Innovation in Imaging, Department of Radiology, Massachusetts General Hospital, Boston, Mass (B.P., C.W., J.W.C.); Department of Radiology, Qilu Hospital of Shandong University, Jinan, China (A.L.); and Department of Radiology, Huashan Hospital, Fudan University, Shanghai, China (A.L., Y.W., X.F., Z.Y.). Received October 28, 2018; revision requested December 3; final revision received June 21, 2019; accepted July 19. **Address correspondence to** J.W.C. (e-mail: *jwchen@mgh.harvard.edu*).

Supported by the National Multiple Sclerosis Society (RG-1507-05486), National Institute of Neurologic Disorders and Stroke (R01-NS070835, R01-NS103998), National Natural Science Foundation of China (81701758), and Natural Science Foundation of Shandong Province (ZR2017BH073).

Conflicts of interest are listed at the end of this article.

See also the editorial by Walczak in this issue.

Radiology 2019; 293:158–165 • https://doi.org/10.1148/radiol.2019182492 • Content codes: MI MR

Background: Despite advances in immunomodulatory agents, most current therapies for multiple sclerosis target lymphocytes or lymphocytic function. However, therapy response may be less than optimal due to demyelination and axonal damage caused by myeloid cells.

Purpose: To determine if myeloperoxidase (MPO) molecular MRI can evaluate whether combination therapy targeting both lymphoid and myeloid inflammation can improve autoimmune neuroinflammation compared with either drug alone, even at suboptimal doses.

Materials and Methods: Four groups of 94 female mice (8–10 weeks old) were induced with experimental autoimmune encephalomyelitis (EAE) from August 2, 2016, to March 30, 2018, and divided into saline control (n = 22), 4-aminobenzoic acid hydrazide (ABAH) therapy group (n = 19), glatiramer acetate (GA) therapy group (n = 22), and combination therapy group (n = 31). Mice were administered suboptimal doses of ABAH, an irreversible inhibitor of MPO; GA, a first-line multiple sclerosis drug; both ABAH and GA; or saline (control). Mice were imaged with *bis*-5-hydroxytryptamide-diethylenetriaminepentaacetate gadolinium (hereafter, MPO-Gd) MRI. One-way analysis of variance, two-way analysis of variance, Kurskal-Wallis, and log-rank tests were used. $P < .05$ was considered to indicate statistical significance.

Results: The combination-treated group showed delayed disease onset (day 11.3 vs day 9.8 for ABAH, day 10.4 for GA, day 9.9 for control; $P < .05$) and reduced disease severity (clinical score during the acute exacerbation period of 1.8 vs 3.8 for ABAH, 3.1 for GA, 3.9 for control; $P < .05$). The combination-treated group demonstrated fewer MPO-positive lesions (30.2 vs 73.7 for ABAH, 64.8 for GA, 67.2 for control; $P < .05$), smaller MPO-positive lesion volume (16.7 mm^3 vs 65.2 mm^3 for ABAH, 69.9 mm^3 for GA, 66.0 mm^3 for control; $P < .05$), and lower intensity of MPO-Gd lesion activation ratio (0.7 vs 1.9 for ABAH, 3.2 for GA, 2.3 for control; $P < .05$). Reduced disease severity in the combination group was confirmed at histopathologic analysis, where MPO expression (1779 vs 2673 for ABAH, 2898 for GA; $P < .05$) and demyelination (5.3% vs 9.0% for ABAH, 10.6% for GA; $P < .05$) were ameliorated.

Conclusion: Myeloperoxidase molecular MRI can track the treatment response from immunomodulatory drugs even if the drug does not directly target myeloperoxidase, and establishes that combination therapy targeting both myeloid and lymphocytic inflammation is effective for murine autoimmune neuroinflammation, even at suboptimal doses.

Online supplemental material is available for this article.

Multiple sclerosis is characterized by the formation of demyelinating lesions and axonal damage in the central nervous system. While the pathogenesis of multiple sclerosis is currently elusive, an inflammatory response induced by lymphocytes, monocytes, and macrophages and microglia is present (1,2). Despite substantial advances in immunomodulatory agents approved for treatment of multiple sclerosis, most of the therapies currently in use were designed to target lymphocytes or lymphocytic function (3,4). However, demyelination and axonal damage are caused by innate immune cells such as monocytes, macrophages, and neutrophils (2,5). Thus, it is not surprising to find that not all patients responded optimally to current therapies (3,6).

Glatiramer acetate (GA), also known as copolymer 1 (Copaxone; Teva Pharmaceuticals, Petach Tikva, Israel) is a first-line immunomodulatory agent approved for treatment of relapsing-remitting multiple sclerosis (3). Its action, among other mechanisms, has been proposed to be associated with a protective T helper type 2–weighted immune response. It induces anti-inflammatory T helper type 2 lymphocytes that gain access to the brain and inhibit the

Abbreviations

ABAH = 4-aminobenzoic acid hydrazide, ANOVA = analysis of variance, EAE = experimental autoimmune encephalitis, GA = glatiramer acetate, MPO = myeloperoxidase

Summary

Molecular MRI of myeloperoxidase tracks changes from immunomodulatory drugs and establishes that combination drug therapy targeting both myeloid and lymphocytic inflammation is effective for autoimmune neuroinflammation in a mouse model, even at suboptimal doses.

Key Results

- By reporting active neuroinflammatory lesions, myeloperoxidase (MPO)-targeted MRI shows that combination therapies for experimental autoimmune neuroinflammation are effective, even using suboptimal doses of drugs (4-aminobenzoic acid hydrazide [ABAH], 20 mg/kg intraperitoneally twice per day; glatiramer acetate [GA], 75 μg subcutaneously once per day) that do not directly target MPO.
- Combination therapy targeting lymphoid and myeloid inflammation (such as using GA and ABAH) showed delayed disease onset (day 11.3 vs ABAH, day 9.8; GA, day 10.4; control, day 9.9; $P < .05$), reduced disease severity (1.8 vs ABAH, 3.8; GA, 3.1; control, 3.9; $P < .05$), fewer MPO-positive lesions (30.2 vs ABAH, 73.7; GA, 64.8; control, 67.2; $P < .05$), smaller MPO-positive lesion volume (16.7 mm^3 vs ABAH, 65.2 mm^3; GA, 69.9 mm^3; control, 66.0 mm^3; $P < .05$), and lower intensity of *bis*-5-hydroxytryptamide-diethylenetriaminepentaacetate gadolinium lesion activation ratio (0.7 vs ABAH, 1.9; GA, 3.2; control, 2.3; $P < .05$).
- Reduced disease severity in the combination group was confirmed at histopathologic analysis, where MPO expression (1779 vs ABAH, 2673; GA, 2898; $P < .05$) and demyelination (5.3% vs ABAH, 9.0%; GA, 10.6%; $P < .05$) were ameliorated.

pathologic inflammatory process (7,8). An irreversible specific inhibitor for myeloperoxidase (MPO) (9), 4-aminobenzoic acid hydrazide (ABAH), is found in active demyelinated plaques in patients with multiple sclerosis (10). MPO is a highly oxidative inflammatory enzyme secreted by monocytes, activated macrophages, microglia, and neutrophils. ABAH inhibition of MPO activity attenuates disease activity in the experimental autoimmune encephalomyelitis (EAE) murine model of multiple sclerosis, resulting in reduced demyelination, tissue damage, and inflammatory cell infiltration with a subsequent improvement in clinical symptoms and mortality (11).

We hypothesized that combination therapy targeting different arms (lymphocytic and myeloid) of the inflammation cascade could yield additional benefits compared with treating either arm alone. By using molecular MRI targeting the inflammatory enzyme MPO, we aimed to determine whether MPO imaging can track treatment effects of immunomodulatory drugs even if the drug does not directly affect myeloid inflammation, and to evaluate whether combination therapy targeting both lymphoid and myeloid inflammation can improve autoimmune neuroinflammation compared with either drug alone, even at suboptimal doses. To track in vivo MPO activity, we used *bis*-5-hydroxytryptamide-diethylenetriaminepentaacetate gadolinium (hereafter, MPO-Gd). MPO-Gd is a specific and sensitive MRI agent for MPO (12–14) correlated with MPO immunostaining (15–17). MPO-Gd helped to detect preclinical and subclinical inflammation that were not identified by using diethylenetriaminepentaacetate gadolinium, or DTPA-Gd (16,18,19). In addition, MPO-Gd imaging correlated better with demyelination compared with DTPA-Gd and reflects the underlying immune response (16).

Materials and Methods

EAE Induction and Treatment Protocol

The protocol for animal experiments was approved by the institutional animal care committee. We induced EAE in 94 Swiss Jim Lambert mice (8–10 weeks old, female; National Cancer Institute, Frederick, Md) with synthetic proteolipid protein (PLP 139–151; Axxora Life Sciences, San Diego, Calif) (17) from August 2, 2016, to March 30, 2018 (A.L., with 2 years of experience in EAE induction). We divided EAE mice into groups of saline control ($n = 22$), ABAH therapy ($n = 19$), GA therapy ($n = 22$), and combination therapy ($n = 31$).

Both GA and ABAH were used at suboptimal doses, because a full dose of either GA or ABAH had already been shown to reduce disease activity such that the synergistic effect of the combination may be masked by the already substantial effect of the full-dose therapy. In a prior study (11), ABAH at a dose of 20 mg/kg was ineffective when injected intraperitoneally twice per day. Similarly, GA was also administered at a suboptimal dose of 75 μg subcutaneously once per day (20). The combination therapy was given as ABAH 20 mg/kg intraperitoneally twice per day, and GA 75 μg subcutaneously once per day. The control group was treated with the same quantity of saline. Treatment started on the day of induction and continued until each mouse was euthanized.

Clinical Scoring

We performed clinical assessment as follows: 0, normal; 1, flaccid tail; 2, unable to use either hind leg; 3, complete paralysis of hindquarters; 4, very weak, unresponsive, and with rapid breathing; 5, moribund. When mice died, they were kept in the trial as a score of 5 for the duration of the study. Information on the scorers are provided in Appendix E1 (online).

Imaging Agent and MPO-Gd Molecular MRI

Previous studies show that MPO is a potential biomarker to monitor active inflammation and demyelination in human multiple sclerosis and animal models of EAE (10,11,17). The specificity of MPO-Gd imaging to help detect MPO activity had been validated in multiple studies in vitro and in vivo, against other peroxidases (21), nonactivatable analog (15), competitive inhibitors (11,18), and in MPO knockout mice (12,14,19,22). MPO-Gd imaging correlates well to MPO histopathologic analysis and demyelination in EAE and other diseases (11,13,14–17,21,22). We synthesized MPO-Gd according to Chen et al (13). We performed MRI ($n = 5$ for control group, $n = 3$ for monotherapy groups, and $n = 5$ for the combination therapy group) on day 10 after induction with a small animal 4.7-T MRI scanner (PharmaScan; Bruker, Billerica, Mass) with a mouse brain coil. We obtained T2-weighted images (repetition time msec/echo time msec, 2811/60; matrix

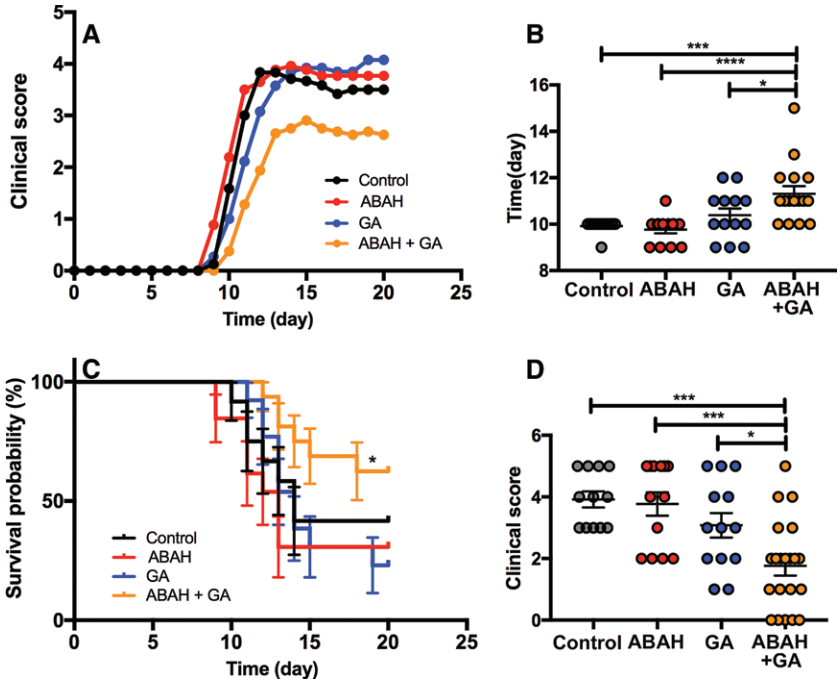

Figure 1: Graphs show experimental autoimmune encephalitis (EAE) with different therapies at suboptimal doses. *A,* Clinical scores over time until day 20 after EAE induction (n = 12 for control, n = 13 for 4-aminobenzoic acid hydrazide [ABAH], n = 13 for glatiramer acetate [GA], n = 16 for combination therapy). *B,* Onset of disease (n = 12 for control, n = 13 for ABAH, n = 13 for GA, n = 16 for combination therapy). *C,* Kaplan-Meier curve of control mice (n = 12) and mice treated with ABAH (n = 13), GA (n = 13), or combination therapy (n = 16). There was improved survival of mice treated with ABAH and GA compared with those treated with ABAH (P = .03) or GA (P = .03). *D,* Clinical scores (maximum clinical score achieved by each mouse) on day 12 during acute exacerbation period (n = 12 for control, n = 13 for ABAH, n = 13 for GA, n = 21 for combination therapy). Swiss Jim Lambert mice (8–10 weeks old, female; National Cancer Institute, Frederick, Md). * = $P < .05$, *** = $P < .001$, **** = $P < .0001$.

size, 256 × 256; field of view, 2.5 × 2.5 cm^2; section thickness, 0.5 mm; 16 sections; 13 minutes) and precontrast T1-weighted images (873/17; matrix size, 192 × 256; field of view, 2.5 × 2.5 cm^2; section thickness, 0.5 mm; 16 sections; 6 minutes for one set of images). After intravenous administration of MPO-Gd (0.3 mmol/kg), with the same sequence as precontrast T1-weighted images, we obtained sequential images (6 minutes for each set of images, continuous 15 sets of images acquired over 90 minutes).

Image analysis.—Three neuroradiologists, including one who is not associated with the study (A.L. and Y.W., with 10 years and 8 years of experience in interpreting images, respectively; average values pertaining to each mouse were used) independently analyzed the images and were blinded to the group and clinical information. MPO-Gd images were quantified by calculating all lesions over the entire brain of each mouse as follows: lesion number, lesion volume, contrast-to-noise ratio, and lesion activation ratio that semiquantitatively reports in vivo MPO activity (11). Three-dimensional image renderings of 90-minute contrast-to-noise ratio maps were performed by manually segmenting the whole brain, an area outside of the mouse (noise), and an area of normal brain on the image 90 minutes after MPO-Gd injection by using commercially available software (Amira, version 5.3.2; ThermoFisher Scientific, Hillsboro, Oreg). Voxel-by-voxel calculation of the contrast-to-noise ratio maps was performed with commercially available software (Matlab R2015a; MathWorks, Natick, Mass). Additional information on the formulas for these computations is available in Appendix E1 (online) .

Histopathologic Analysis

Fresh-frozen 6-μm brain slices were examined for demyelination and MPO protein. Additional information is available in Appendix E1 (online).

Isolation of Brain Inflammatory Cells and Flow Cytometry

We extracted leukocytes from the brain over a discontinuous Percoll gradient, as previously described (16). The gating strategy is illustrated in Figure E1 (online). Additional information is available in Appendix E1 (online).

Statistical Analysis

Results were reported as means ± standard error of measurement. The data were tested for normality by using the Shapiro-Wilk normality test. We performed one-way analysis of variance (ANOVA) (histopathologic analysis of MPO), two-way ANOVA (lesion number, lesion volume, contrast-to-noise ratio, and lesion activation ratio for MRI images; flow cytometry), and nonparametric Kruskal-Wallis test (onset of disease, clinical score on day 12, histopathologic analysis of luxol fast blue stain). For survival analysis, we used Kaplan-Meier curve and log-rank test. $P < .05$ was considered to indicate statistical significance. Commercially available software (Prism, version 7; GraphPad Software, San Diego, Calif) was used for statistical analysis. Additional information is available in Appendix E1 (online).

Results

Combination Therapy Ameliorated Clinical EAE

We followed the mice up to day 20 after EAE induction (Fig 1, *A*). At the suboptimal doses used, mice treated with the combination therapy developed EAE symptoms later (mean ± standard error of measurement, 11.3 days ± 0.3; n = 16; Kruskal-Wallis test) compared with ABAH-treated (mean, 9.8 days ± 0.2; $P < .0001$; n = 13), GA-treated (mean, 10.4 days ± 0.3; P = .04; n = 13), and control mice (mean, 9.9 days ± 0.1; $P < .001$; n = 12) (Fig 1, *B*). Combination therapy tended to improve survival, with survival rate of 62.5% (10 of 16) compared with that of suboptimal ABAH treatment at 30.8% (four of 13; median survival, 13 days; P = .03), suboptimal GA treatment at 23.1% (three of 13; median survival, 14 days; P = .03), and control group at 41.7% (five of 12; median sur-

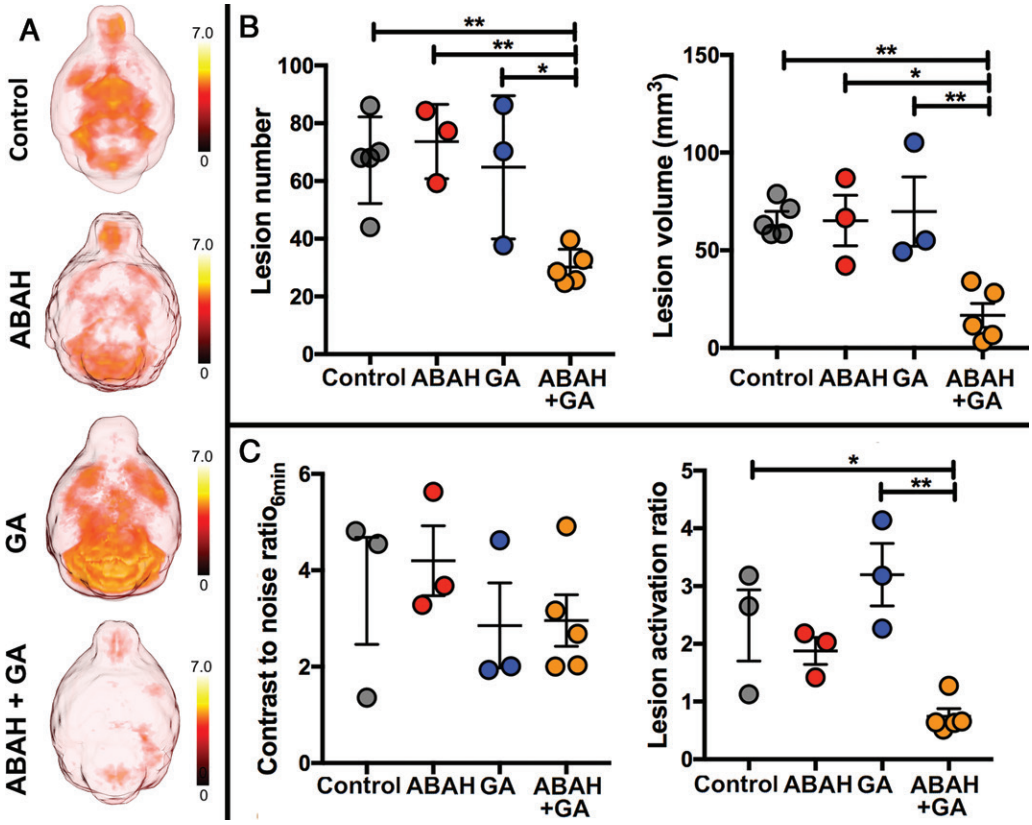

Figure 2: Images show myeloperoxidase (MPO)-specific MRI of treatment effect. *A,* Representative three-dimensional maps of 90-minute *bis*-5-hydroxytryptamide-diethylenetriaminepentaacetate gadolinium (hereafter, MPO-Gd) contrast-to-noise ratios (CNRs) over entire brain (axial view) show overall disease burden for each group. *B,* Average lesion number and lesion volume (on day 10, the acute exacerbation period; $n = 5$ in control group, $n = 3$ in single therapy group, $n = 5$ in combination therapy group). *C,* Early CNRs at 6 minutes after MPO-Gd injection ($n = 3$ in control group, $n = 3$ in single therapy group, $n = 5$ in combination therapy group) and MPO-specific lesion activation ratios ($n = 3$ in control group, $n = 3$ in single therapy group, $n = 5$ in combination therapy group). Swiss Jim Lambert mice (8–10 weeks old, female; National Cancer Institute, Frederick, Md). ABAH = 4-aminobenzoic acid hydrazide, GA = glatiramer acetate. * = $P < .05$, ** = $P < .01$.

vival, 14 days; $P = .16$) (Fig 1, *C*; Fig E2 [online]). When calculating the maximum clinical score achieved by each mouse on day 12 during the acute exacerbation period, the mice treated with combination therapy showed improved clinical scores during the acute exacerbation period (Kruskal-Wallis test; mean, 1.8 ± 0.3; $n = 21$ vs ABAH: mean, 3.8 ± 0.4; $P < .001$; $n = 13$ vs GA: mean, 3.1 ± 0.4; $P = .03$; $n = 13$ vs control group: mean, 3.9 ± 0.3; $P < .001$; $n = 12$) (Fig 1, *D*).

Combination Therapy Reduced Active Inflamed Plaques in Vivo

In the control mice and in mice with suboptimal ABAH or GA treatment, there were widespread MPO-positive lesions throughout the brain but markedly fewer such lesions in the brains of mice treated with combination therapy (Fig 2, *A*). There was marked reduction in other imaging metrics of active disease with the combination therapy (Fig 2, *B* and *C*). During the acute exacerbation period, there were fewer lesions in mice treated with combination therapy (mean, 30.2 ± 2.7; $n = 5$; two-way ANOVA) than in mice treated with single therapy (ABAH: mean, 73.7 ± 7.4; $P = .008$; $n = 3$; GA: mean, 64.8 ± 14.3; $P = .03$; $n = 3$), and control mice (mean, 67.2 ± 6.7; $P = .009$; $n = 5$ (Fig 2, *B*; left). The total lesion volume was also smaller in mice treated with combination therapy (16.7 mm^3 ± 6.1; $n = 5$; two-way ANOVA) than in mice treated with single therapy (ABAH: mean, 65.2 mm^3 ± 12.9; $P = .02$; $n = 3$; GA: mean, 69.9 mm^3 ± 17.8; $P = .008$; $n = 3$) and control mice (mean, 66.0 mm^3 ± 4.0; $P = .005$; $n = 5$) (Fig 2, *B*; right).

The early postcontrast contrast-to-noise ratios at 6 minutes after MPO-Gd injection reflects leakage of the agent across a compromised blood-brain barrier, and behaves similar to that of DTPA-Gd. This measure was unable to identify whether the combination therapy (mean, 3.0 ± 0.5; $n = 5$; two-way ANOVA) was more effective compared with the monotherapy and control group (ABAH: mean, 4.2 ± 0.7; $P = .66$; $n = 3$; GA: mean, 2.9 ± 0.9; $P = .99$; $n = 3$; control: mean, 3.6 ± 1.1; $P = .94$; $n = 3$ (Fig 2, *C*; left). However, when we compared the MPO-specific lesion activation ratio, there was lower lesion activation ratio for the combination-treated mice compared with the monotherapy groups and control group (two-way ANOVA; mean, 0.7 ± 0.1; $n = 5$ for combination vs mean, 1.9 ± 0.2 for ABAH; $P = .17$; $n = 3$ vs mean, 3.2 ± 0.5 for GA; $P = .003$; $n = 3$ vs mean, 2.3 ± 0.6 for control; $P = .04$; $n = 3$ (Fig 2, *C*; right), revealing reduced activation of MPO-Gd in the combination-treated mice.

Histopathologic and Flow Cytometry Outcomes

As expected from prior studies (11,17), MPO-Gd enhancement matched well with MPO and histopathologic analysis with luxol fast blue (Fig 3). There was widespread MPO staining in the suboptimal GA-treated group (mean, 2898 ± 357.7; $P = .01$; $n = 7$) and ABAH-treated group (mean, 2673 ± 168.4; $P = .05$; $n = 7$) and a lesser amount of MPO staining in the mice treated with combination therapy (mean, 1779 ± 208.5; $n = 7$; one-way ANOVA) (Fig 4). Similarly, demyelination was more attenuated in the mice treated with combination therapy (mean, 5.3% ± 0.5; $n = 6$; Kruskal-Wallis test) than in both suboptimal ABAH-treated (mean, 9.0% ± 0.8; $P = .03$; $n = 6$) and suboptimal GA-treated mice (mean, 10.6% ± 1.5; $P = .05$; $n = 6$ (Fig 4).

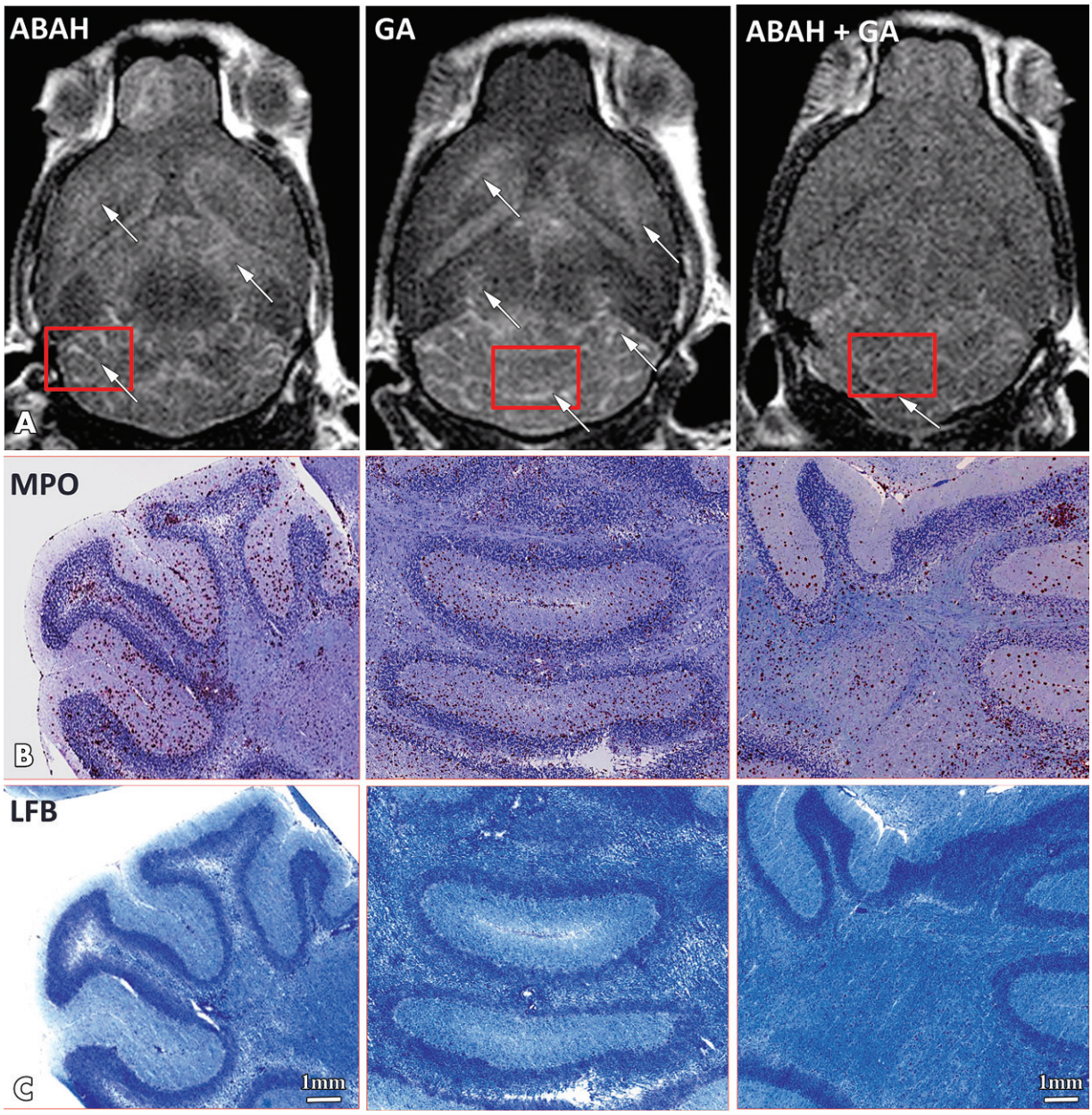

Figure 3: Images show correlation of myeloperoxidase (MPO)-specific MRI with histopathologic analysis for MPO and demyelination. *A,* Representative late (90-minute) brain MRI (axial plane) for MPO-specific enhancing lesions (white arrow) throughout brain in suboptimally treated mice with 4-aminobenzoic acid hydrazide (ABAH), glatiramer acetate (GA), or combination therapy. Corresponding histopathologic slices (red rectangles) of, *B,* MPO immunostaining and, *C,* myelination (luxol fast blue [LFB]; blue areas represent intact myelin and white areas are demyelinated) in mice treated with ABAH, GA, or combination therapy. Scale bar = 1 mm; original magnification, ×1.25. Swiss Jim Lambert mice (8–10 weeks old, female; National Cancer Institute, Frederick, Md).

We also profiled for macrophages and microglia, proinflammatory monocytes, neutrophils, and lymphocytes in the brain by using flow cytometry to assess whether the treatments changed the immune cell populations (Fig E3 [online]). We found no difference in the number of macrophages and microglia between the four groups (mean, 60.4% ± 4.8; n = 5 for combination therapy vs mean, 44.7% ± 7.9 for ABAH; P = .18; n = 3 vs mean, 47.7% ± 3.0 for GA; P = .20 n = 6 vs mean, 53.4% ± 4.3 for control; P = .69; n = 5 (Fig E3a [online]). We found fewer proinflammatory monocytes (Ly-6C^{hi}/F4/80^{low}, or cell population with high expression of Ly-6C and low expression of F4/80) in the combination group than in the control group (two-way ANOVA; mean, 1.4% ± 0.2 for combination; n = 5 vs mean, 2.7% ± 0.4 for control; P = .046; n = 5) (Fig E3b [online]), but did not find a difference between the combination group and single therapy groups (two-way ANOVA; mean, 1.4% ± 0.2 for combination; n = 5 vs mean, 2.1% ± 0.1 for ABAH; P = .58; n = 3 vs mean, 2.2% ± 0.4 for GA; P = .25; n = 6) (Fig E3b [online]). We found no difference between all four groups for neutrophils (two-way ANOVA; mean, 3.9% ± 0.5 for combination; n = 5 vs mean, 4.8% ± 1.0 for ABAH; P = .85; n = 3 vs mean, 3.6% ± 0.5 for GA; P = .99; n = 6 vs mean, 3.9% ± 0.9

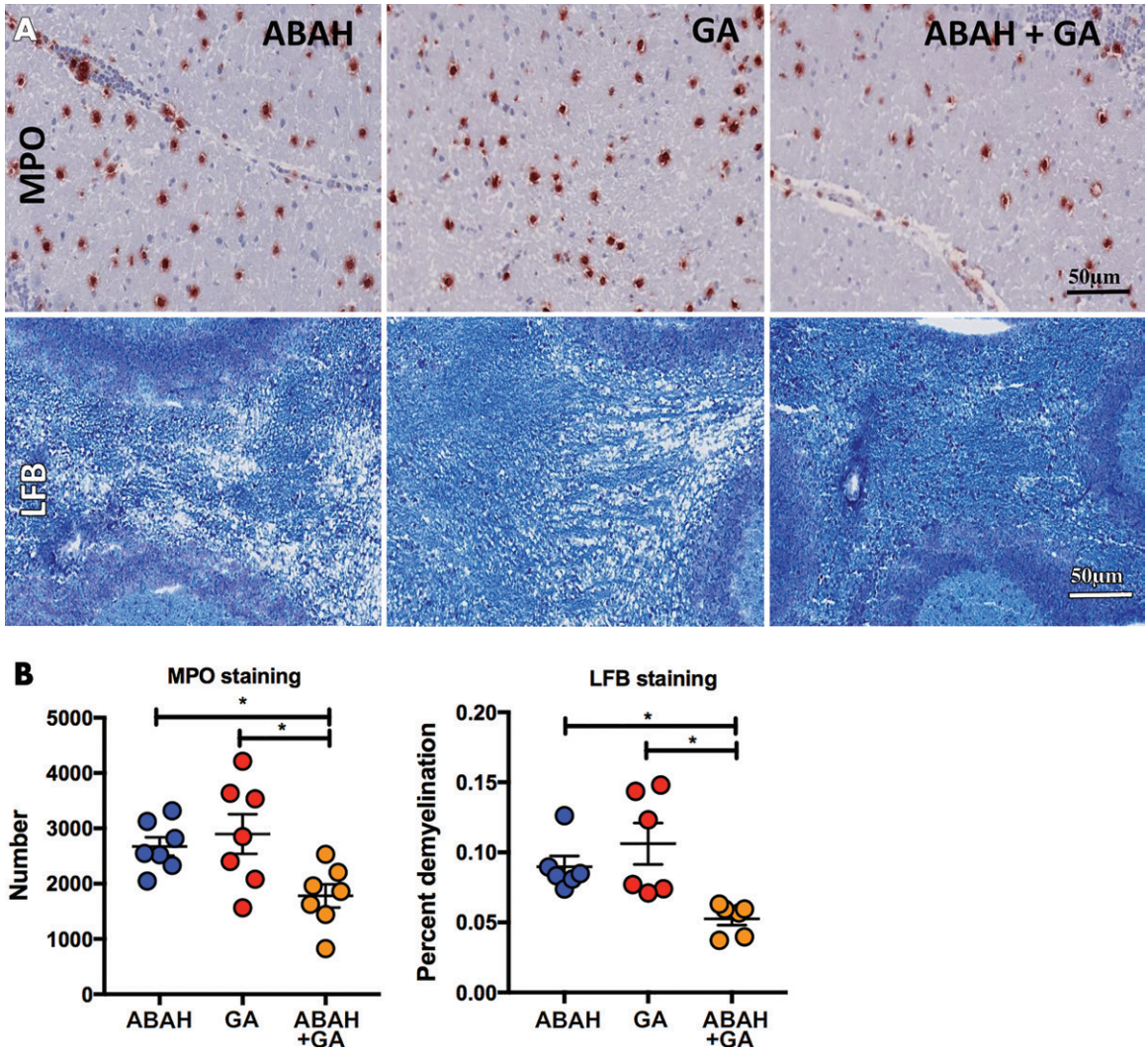

Figure 4: Images show histopathologic analyses of myeloperoxidase (MPO) and myelination. *A,* Representative high-magnification immunohistochemical slices of MPO staining and myelination (luxol fast blue [LFB]; blue areas represent intact myelin and white areas are demyelinated). *B,* Quantification of MPO in mice treated with 4-aminobenzoic acid hydrazide (ABAH) (*n* = 7), glatiramer acetate (GA) (*n* = 7), and combination therapy (*n* = 7); demyelination in mice treated with ABAH (*n* = 6), GA (*n* = 6), and combination therapy (*n* = 6). Scale bar = 50 μm; original magnification, ×50. Swiss Jim Lambert mice (8–10 weeks old, female; National Cancer Institute, Frederick, Md). ∗ = $P < .05$.

for control; $P > .99$; $n = 5$) (Fig E3c [online]) and lymphocytes (two-way ANOVA; mean, 24.8% ± 5.1 for combination; n = 5 vs mean, 38.6% ± 10.4 for ABAH; $P = .34$; $n = 3$ vs mean, 39.2% ± 2.6 for GA; $P = .18$; $n = 6$ vs mean, 33.8% ± 4.6 for control; $P = .58$; $n = 5$) (Fig E3d [online]). Although nonsignificant, there appeared to be a lower number of lymphocytes in the combination-treated groups compared with the other groups (Fig E3d [online]).

Discussion

Most current therapies for multiple sclerosis target lymphocytes or lymphocytic function. However, response may be less than optimal due to damage caused by innate immune cells. In this study, we established that combination drug therapy targeting both myeloid and lymphocytic inflammation is effective for autoimmune neuroinflammation in a mouse model, even at suboptimal doses. By using myeloperoxidase (MPO) as a biomarker for active inflammation, we found that this synergistic benefit could be noninvasively tracked with MRI, demonstrating a lower number of MPO-positive lesions, smaller lesion volume, and a reduced amount of MPO-mediated enhancement with the combination therapy than with either drug alone or the control group. The reduced demyelination and MPO protein at neuropathologic analysis further corroborated the synergistic benefits. Our data illustrated that molecular imaging with *bis*-5-hydroxytryptamide-diethylenetriaminepentaacetate gadolinium (hereafter, MPO-Gd) can track the effects of immunomodulatory drugs even if the drugs do not specifically affect MPO. This is likely due to MPO being a downstream effector molecule of inflammation, thus allowing MPO-Gd to sense changes from upstream modulations. No unexpected adverse events occurred when applying the two drugs together.

In our study, molecular MRI of MPO played a key role in the evaluation of the different therapies. Previous studies have compared MPO-Gd with diethylenetriaminepentaacetate gadolinium, or DTPA-Gd, in several animal models including experimental

autoimmune encephalitis (EAE) (12,14–19). In MPO-Gd imaging, early contrast-to-noise ratios (6 minutes) are indicative of leakage across the blood-brain barrier prior to agent activation and retention and are similar to DTPA-Gd imaging. Late contrast-to-noise ratios (90 minutes) and lesion activation ratio reveal signal from MPO-mediated activation and retention of activated MPO-Gd and is sensitive and specific to MPO activity. Thus, in our study, early nonspecific postcontrast images at 6 minutes were not able to distinguish between the groups. However, in vivo MPO activity assessed by lesion activation ratio was able to report the synergistic benefit of the combination therapy.

One recent study by Zhang et al (23) used both MPO-Gd MRI and MMPSense 680 (PerkinElmer, Waltham, Mass) fluorescence molecular tomography imaging in EAE. They used full-dose 4-aminobenzoic acid hydrazide (ABAH) to study mechanistic effect of MPO on matrix metalloproteinase. Our study used suboptimal dose of ABAH alone or in combination with suboptimal dose of glatiramer acetate (GA). In the study by Zhang et al (23), MPO-Gd was used to confirm that MPO activity was suppressed by ABAH, with the primary readout being fluorescent imaging of matrix metalloproteinase activity. We used MPO-Gd imaging as the primary means to assess whether suboptimal monotherapy or combination therapy affected brain inflammation. To our knowledge, ABAH has not been directly administered to humans or patients with multiple sclerosis, although some prior studies have used ABAH in human samples (24,25). Nonetheless, MPO inhibition reduces inflammation in multiple disease models, and several companies are developing potent MPO inhibitors (26,27).

Our study had limitations. We did not image the mice at peak clinical illness (day 13–15), because lesion load at imaging can precede clinical illness (17). At peak clinical illness, blood-brain barrier breakdown and lesion burden may already be declining and be potentially misleading. Furthermore, not all mice survived to day 13–15, particularly in the monotherapy groups, which would bring in a bias toward healthier mice if evaluated at a time when sicker mice in a group have already died. It should be noted there is substantial substrain difference in susceptibility to EAE (28), with mice from Charles River Laboratories (Wilmington, Mass) being the most susceptible and those from the Jackson Laboratory (Bar Harbor, Maine) the least susceptible. Although mice from the National Cancer Institute have not been tested in literature, we found National Cancer Institute mice showed a higher disease severity and mortality than did those from Charles River Laboratories. Because of this, the scores remained high in the later period of our study, although the remaining mice did remit and some started to relapse. The monotherapy groups appear to exhibit slightly worse disease course and mortality compared with those of the control group. These differences were not significant and likely due to statistical noise, given that we did not find alteration to the immune response between these groups at flow cytometry. Nonetheless, it is possible that there may be subtle changes that we did not uncover in the immune response.

In conclusion, our results showed that molecular imaging targeting myeloperoxidase can be used to evaluate immunomodulatory therapies, and established that combination therapy with drugs that targets both myeloid and lymphocytic inflammation is a potential effective therapy for autoimmune neuroinflammation at reduced doses and potential toxicities. Interestingly, only combination therapy decreased proinflammatory monocytes. Although beyond the scope of this work, this suggests that the two drugs acted in synergy: as 4-aminobenzoic acid hydrazide partially reduces the proinflammatory response caused by myeloperoxidase, this may have allowed glatiramer acetate–induced T helper type 2 cells to more effectively block the recruitment of additional proinflammatory monocytes, given that T helper type 2 cells have been found to decrease monocyte chemoattractant protein-1 (29). Future work to reveal additional mechanistic insight into how these treatment regimens affected myeloid and lymphocytic inflammation would be valuable in the development of therapeutic options.

Author contributions: Guarantors of integrity of entire study, A.L., Y.W., Z.Y., J.W.C.; study concepts/study design or data acquisition or data analysis/interpretation, all authors; manuscript drafting or manuscript revision for important intellectual content, all authors; approval of final version of submitted manuscript, all authors; agrees to ensure any questions related to the work are appropriately resolved, all authors; literature research, A.L., B.P., G.R.W., J.H.L., X.F., Z.Y., J.W.C.; experimental studies, A.L., Y.W., B.P., G.R.W., Y.I., C.W., J.H.L., M.A., J.W.C.; statistical analysis, A.L., B.P., G.R.W., J.W.C.; and manuscript editing, A.L., B.P., G.R.W., C.W., J.H.L., M.A., Z.Y., J.W.C.

Disclosures of Conflicts of Interest: A.L. disclosed no relevant relationships. **Y.W.** disclosed no relevant relationships. **B.P.** Activities related to the present article: institution received a research resident grant from the Radiological Society of North America. Activities not related to the present article: disclosed no relevant relationships. Other relationships: disclosed no relevant relationships. **G.R.W.** disclosed no relevant relationships. **Y.I.** disclosed no relevant relationships. **C.W.** disclosed no relevant relationships. **J.H.L.** disclosed no relevant relationships. **M.A.** disclosed no relevant relationships. **X.F.** disclosed no relevant relationships. **Z.Y.** disclosed no relevant relationships. **J.W.C.** Activities related to the present article: disclosed no relevant relationships. Activities not related to the present article: is a consultant for Bayer; is employed by Massachusetts General Hospital; institution receives royalties from Elsevier. Other relationships: institution receives money for patent issued in 2011 for imaging enzymatic activity.

References

1. Frohman EM, Racke MK, Raine CS. Multiple sclerosis: the plaque and its pathogenesis. N Engl J Med 2006;354(9):942–955.
2. Sospedra M, Martin R. Immunology of multiple sclerosis. Annu Rev Immunol 2005;23(1):683–747.
3. Johnson KP, Brooks BR, Cohen JA, et al. Copolymer 1 reduces relapse rate and improves disability in relapsing-remitting multiple sclerosis: results of a phase III multicenter, double-blind placebo-controlled trial. The Copolymer 1 Multiple Sclerosis Study Group. Neurology 1995;45(7):1268–1276.
4. Polman CH, O'Connor PW, Havrdova E, et al. A randomized, placebo-controlled trial of natalizumab for relapsing multiple sclerosis. N Engl J Med 2006;354(9):899–910.
5. Ransohoff RM. How neuroinflammation contributes to neurodegeneration. Science 2016;353(6301):777–783.
6. Paty DW, Li DK. Interferon beta-1b is effective in relapsing-remitting multiple sclerosis. II. MRI analysis results of a multicenter, randomized, double-blind, placebo-controlled trial. UBC MS/MRI Study Group and the IFNB Multiple Sclerosis Study Group. Neurology 1993;43(4):662–667.
7. Weber MS, Starck M, Wagenpfeil S, Meinl E, Hohlfeld R, Farina C. Multiple sclerosis: glatiramer acetate inhibits monocyte reactivity in vitro and in vivo. Brain 2004;127(Pt 6):1370–1378.
8. Weber MS, Prod'homme T, Youssef S, et al. Type II monocytes modulate T cell-mediated central nervous system autoimmune disease. Nat Med 2007;13(8):935–943.
9. Kettle AJ, Gedye CA, Hampton MB, Winterbourn CC. Inhibition of myeloperoxidase by benzoic acid hydrazides. Biochem J 1995;308(Pt 2):559–563.
10. Gray E, Thomas TL, Betmouni S, Scolding N, Love S. Elevated activity and microglial expression of myeloperoxidase in demyelinated cerebral cortex in multiple sclerosis. Brain Pathol 2008;18(1):86–95.
11. Forghani R, Wojtkiewicz GR, Zhang Y, et al. Demyelinating diseases: myeloperoxidase as an imaging biomarker and therapeutic target. Radiology 2012;263(2):451–460.
12. Breckwoldt MO, Chen JW, Stangenberg L, et al. Tracking the inflammatory response in stroke in vivo by sensing the enzyme myeloperoxidase. Proc Natl Acad Sci U S A 2008;105(47):18584–18589.

13. Chen JW, Querol Sans M, Bogdanov A Jr, Weissleder R. Imaging of myeloperoxidase in mice by using novel amplifiable paramagnetic substrates. Radiology 2006;240(2):473–481.
14. Nahrendorf M, Sosnovik D, Chen JW, et al. Activatable magnetic resonance imaging agent reports myeloperoxidase activity in healing infarcts and noninvasively detects the antiinflammatory effects of atorvastatin on ischemia-reperfusion injury. Circulation 2008;117(9):1153–1160.
15. Ronald JA, Chen JW, Chen Y, et al. Enzyme-sensitive magnetic resonance imaging targeting myeloperoxidase identifies active inflammation in experimental rabbit atherosclerotic plaques. Circulation 2009;120(7):592–599.
16. Pulli B, Bure L, Wojtkiewicz GR, et al. Multiple sclerosis: myeloperoxidase immunoradiology improves detection of acute and chronic disease in experimental model. Radiology 2015;275(2):480–489.
17. Chen JW, Breckwoldt MO, Aikawa E, Chiang G, Weissleder R. Myeloperoxidase-targeted imaging of active inflammatory lesions in murine experimental autoimmune encephalomyelitis. Brain 2008;131(Pt 4):1123–1133.
18. Rashid I, Maghzal GJ, Chen YC, et al. Myeloperoxidase is a potential molecular imaging and therapeutic target for the identification and stabilization of high-risk atherosclerotic plaque. Eur Heart J 2018;39(35):3301–3310.
19. Pulli B, Wojtkiewicz G, Iwamoto Y, et al. Molecular MR imaging of myeloperoxidase distinguishes steatosis from steatohepatitis in nonalcoholic fatty liver disease. Radiology 2017;284(2):390–400.
20. Aharoni R, Herschkovitz A, Eilam R, et al. Demyelination arrest and remyelination induced by glatiramer acetate treatment of experimental autoimmune encephalomyelitis. Proc Natl Acad Sci U S A 2008;105(32):11358–11363.
21. Rodríguez E, Nilges M, Weissleder R, Chen JW. Activatable magnetic resonance imaging agents for myeloperoxidase sensing: mechanism of activation, stability, and toxicity. J Am Chem Soc 2010;132(1):168–177.
22. Swirski FK, Wildgruber M, Ueno T, et al. Myeloperoxidase-rich Ly-6C+ myeloid cells infiltrate allografts and contribute to an imaging signature of organ rejection in mice. J Clin Invest 2010;120(7):2627–2634.
23. Zhang Y, Dong H, Seeburg DP, et al. Multimodal molecular imaging demonstrates myeloperoxidase regulation of matrix metalloproteinase activity in neuroinflammation. Mol Neurobiol 2019;56(2):954–962.
24. Békési G, Kakucs R, Sándor J, et al. Plasma concentration of myeloperoxidase enzyme in pre- and post-climacterial people: related superoxide anion generation. Exp Gerontol 2001;37(1):137–148.
25. Han L, Shen X, Pan L, et al. Aminobenzoic acid hydrazide, a myeloperoxidase inhibitor, alters the adhesive properties of neutrophils isolated from acute myocardial infarction patients. Heart Vessels 2012;27(5):468–474.
26. Churg A, Marshall CV, Sin DD, et al. Late intervention with a myeloperoxidase inhibitor stops progression of experimental chronic obstructive pulmonary disease. Am J Respir Crit Care Med 2012;185(1):34–43.
27. Zheng W, Warner R, Ruggeri R, et al. PF-1355, a mechanism-based myeloperoxidase inhibitor, prevents immune complex vasculitis and anti-glomerular basement membrane glomerulonephritis. J Pharmacol Exp Ther 2015;353(2):288–298.
28. deLuca LE, Pikor NB, O'Leary J, et al. Substrain differences reveal novel disease-modifying gene candidates that alter the clinical course of a rodent model of multiple sclerosis. J Immunol 2010;184(6):3174–3185.
29. Yano S, Yanagawa H, Nishioka Y, Mukaida N, Matsushima K, Sone S. T helper 2 cytokines differently regulate monocyte chemoattractant protein-1 production by human peripheral blood monocytes and alveolar macrophages. J Immunol 1996;157(6):2660–2665.